

CONDENSED MATTER PHYSICS

Topological bootstrap: Fractionalization from Kondo coupling

Timothy H. Hsieh,^{1*} Yuan-Ming Lu,² Andreas W. W. Ludwig³

Topologically ordered phases of matter can host fractionalized excitations known as “anyons,” which obey neither Bose nor Fermi statistics. Despite forming the basis for topological quantum computation, experimental access to these exotic phases has been very limited. We present a new route toward realizing fractionalized topological phases by literally building on unfractioalized phases, which are much more easily realized experimentally. Our approach involves a Kondo lattice model in which a gapped electronic system of noninteracting fermions is coupled to local moments via the exchange interaction. Using general entanglement-based arguments and explicit lattice models, we show that gapped spin liquids can be induced in the spin system, and we demonstrate the power of this “topological bootstrap” by realizing chiral and Z_2 spin liquids. This technique enables the realization of many long sought-after fractionalized phases of matter.

INTRODUCTION

The discoveries of the integer and fractional quantum Hall effects have, respectively, ballooned during the last decade into two broad classes of topological phases, distinguished by whether or not fractional excitations exist in the bulk. The integer quantum Hall variety has given rise to “symmetry-protected topological” (SPT) phases (1–3), which cannot be adiabatically deformed into a direct product state as long as certain symmetries are preserved. In contrast, the fractional quantum Hall variety exhibits “intrinsic topological order” (4), manifested by fractionalized bulk excitations obeying anyonic statistics, ground-state degeneracy on a torus, and, in many cases, gapless boundary modes.

Despite their common origin of quantum Hall systems, these two classes have differed significantly in terms of experimental accessibility. The SPT variety has been realized in numerous materials and experimental systems. These include topological insulators protected by time reversal symmetry (5) and topological crystalline insulators (6) protected by mirror symmetry (7), spanning different material classes that are realizable at room temperature. In contrast, intrinsic topological orders have been limited to fractional quantum Hall systems (8) and quantum spin liquids (QSLs) in frustrated magnets (9). Given the importance of intrinsic topological order in enabling topological quantum computation (10, 11), a new route for realizing intrinsic topological orders is highly desirable.

Here, we establish a general “topological bootstrap” scheme in which an unfractioalized phase is used to induce a fractionalized phase via Kondo coupling. This powerful machinery allows us to construct a large class of interacting lattice models, whose ground states realize “projected wave functions” (12–16) for intrinsic topological orders. These have been extensively used as variational wave functions for topological orders, despite the lack of parent microscopic models—a gap filled by the topological bootstrap. To achieve this, we leverage aspects of the bulk topological proximity effect introduced by Hsieh *et al.* (17), in which a free-fermion topological phase in system A induces the “inverse” topological phase in a proximate system B.

The topological bootstrap construction has sharply defined experimental signatures. Our primary example is a Chern insulator for spin-

up and spin-down electrons, coupled to a system of noninteracting spins (Fig. 1A). Before coupling, the Chern insulator has edge modes carrying both spin and charge. The Kondo coupling induces a chiral spin liquid (CSL) in the spin system, with a spin-carrying edge mode of chirality opposite to the Chern insulator. As a result, the counterpropagating spin modes gap out, leaving only a charge mode at the boundary (Fig. 1B). In contrast, for a terrace geometry illustrated in Fig. 1C, the counterpropagating spin mode induced in the spin system is spatially separated from the edge of the electron system and thus can be detected independently.

The structure of this article is as follows. First, we will provide general arguments motivating the topological bootstrap. After firmly establishing these arguments within an entanglement-based approach, we will provide a concrete lattice model in which we show exactly that the topological bootstrap realizes a Z_2 spin liquid induced from a free-fermion superconductor. Finally, we present two lattice models in which a CSL is induced from a Chern insulator.

RESULTS

The bulk topological proximity effect considered by Hsieh *et al.* (17) involves two free-fermion systems, A and B, with different Hamiltonians: H_A has a gap Δ_A and a topologically nontrivial ground state $|\psi_0^A\rangle$, whereas $H_B = 0$ corresponds to a system of decoupled fermion degrees of freedom. The two systems are extensively coupled to each other via a local tunneling term, which favors maximal entanglement of the degrees of freedom on the corresponding lattice sites of systems A and B. See (18) for an entanglement perspective on the bulk topological proximity effect. After coupling, system B perfectly “screens” system A by developing the inverse topological phase: For example, a band insulator with Chern number +1 induces a Chern number –1 state in B after the two are coupled. More precisely, the composite ground state, as obtained in degenerate perturbation theory in g , the strength of coupling, is of the form $|\psi_0\rangle = |\psi_0^A\rangle|\psi_0^B\rangle + O(g/\Delta_A)$, where the bar denotes the inverse topological phase (such that the composite system is topologically trivial).

What if systems A and B have different degrees of freedom, such as free fermions in A and spins in B? In this case, it is impossible for B to fully screen A because of the mismatch of Hilbert spaces. However, a partial screening of spin degrees of freedom can induce even more interesting topological phases in system B, as will become evident below.

Copyright © 2017
The Authors, some
rights reserved;
exclusive licensee
American Association
for the Advancement
of Science. No claim to
original U.S. Government
Works. Distributed
under a Creative
Commons Attribution
NonCommercial
License 4.0 (CC BY-NC).

¹Kavli Institute for Theoretical Physics, University of California Santa Barbara, CA 93106, USA. ²Department of Physics, The Ohio State University, Columbus, OH 43210, USA. ³Department of Physics, University of California Santa Barbara, CA 93106, USA.

*Corresponding author. Email: thsieh@kitp.ucsb.edu

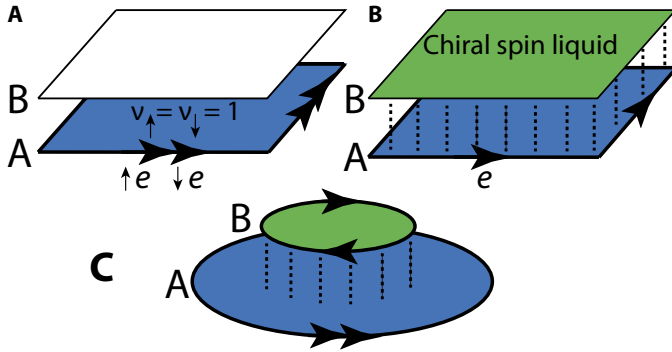


Fig. 1. Example and phenomenology of topological bootstrap. (A) Two decoupled layers: a Chern insulator (blue, A) and a free layer of spins (white, B). *e*, electron. (B) After Kondo coupling, the Chern insulator induces a CSL (green) with the opposite chirality. The counterpropagating spin modes gap out, leaving a charge mode. (C) In a terrace construction, the induced and original edge modes are widely separated and coexist.

Our construction involves composite systems in which A is a topological phase of noninteracting fermions and B consists of decoupled spins residing on the same sites as the fermions. In particular, we consider a Kondo lattice model in which the electron system is a topological band insulator or a gapped superconductor, as opposed to a metal. The intuition from the topological proximity effect is that although the spins cannot perfectly screen the fermions by forming the inverse topological phase, they are expected to inherit the spin sector of the free-fermion system. More precisely, in a slave-fermion description of the spins ($\vec{S} = \frac{1}{2}f^\dagger \vec{\sigma} f$), the *f* fermions would form the inverse phase with respect to A, leading to a QSL state described by a Gutzwiller-projected wave function in system B. Because the electron system is gapped with zero density of states, we expect that Kondo singlet formation is evaded at weak coupling ($g \ll \Delta_A$), and the above physics is described by a new Kondo mean-field theory with a topologically ordered ground state.

We will illustrate the topological bootstrap in the simplest scenario of a two-dimensional bilayer: A is a system of noninteracting fermions at half-filling with both spin-up and spin-down electrons $c_{\uparrow/\downarrow}$ each in a Chern number 1 band, and B is a system of decoupled spin- $1/2$'s with one spin- $1/2$ per site. The composite Hamiltonian is

$$H = H_0 + H_K \tag{1}$$

$$= H_{v=1}(c_\uparrow) + H_{v=1}(c_\downarrow) + g \sum_i (c_i^\dagger \vec{\sigma} c_i) \cdot \vec{S}_i \tag{2}$$

where H_K represents an antiferromagnetic Kondo coupling between fermions and localized spins, parametrized by $g \geq 0$. (Here, “*i*” denotes lattice sites.) We will see that the state in the spin system B will be in the same phase as the Gutzwiller projection of the Chern number 1 state, enforcing one fermion per site. This is known to be a CSL (19, 20), having intrinsic topological order with fractionalized “semi-” excitations in the bulk and chiral edge states.

It is useful to directly relate the above Kondo model to the free-fermion topological proximity effect. In particular, we can begin with a free-fermion model

$$H_{v=1}(c_\uparrow) + H_{v=1}(c_\downarrow) + v \sum_{i, \sigma=\uparrow, \downarrow} c_{i, \sigma}^\dagger f_{i, \sigma} + h.c.$$

in which the Chern insulator is now coupled to “Kondo fermions” f_σ via a tunneling term of strength *v*. In the study by Hsieh *et al.* (17), it was found that for any value of *v*, the composite system is always gapped and topologically trivial. In other words, an $SU(2)$ -symmetric Chern insulator of opposite chirality is induced in the system of Kondo fermions by an arbitrarily small coupling *v*. Consider a coupling *v* much smaller than the band gap Δ_A of the Chern insulator; then, a hopping term of Kondo fermions of the order $t \approx v^2/\Delta_A$ is induced.

Now, we add an on-site Hubbard interaction

$$U \sum_i (f_{i, \uparrow}^\dagger f_{i, \uparrow} + f_{i, \downarrow}^\dagger f_{i, \downarrow} - 1)^2 \tag{3}$$

for Kondo fermions. In the parameter range $t \ll U \ll v \ll \Delta_A$, the low-energy physics of the Kondo fermions (which are at half-filling) can be described by localized spins \vec{S}_i , and we recover the original Kondo model (Eq. 2) with effective Kondo coupling $g \sim v^2/\sqrt{U\Delta_A}$. Thus, we expect that the state induced in the spin system B via our Kondo setup is related to the physics of Chern bands with Hubbard interactions, where CSLs have been found in previous works (21). We now support this intuition with both an entanglement argument and microscopic lattice models.

Entanglement arguments

The key feature of the antiferromagnetic Kondo coupling term \hat{H}_K in Eq. 2 is that its ground state is a direct product of singlets

$$\begin{aligned} |\Psi_{AB}\rangle &= \prod_i \left[\frac{1}{\sqrt{2}} \sum_{\sigma_i = \pm \frac{1}{2}} \text{sgn}(\sigma_i) c_{i, \sigma_i}^\dagger |0\rangle_A \otimes |\mathcal{S}_i^\sigma = -\sigma_i\rangle_B \right] \\ &= \frac{1}{\sqrt{2^N}} \sum_{\{\sigma_i\}} \left(\prod_i \text{sgn}(\sigma_i) \right) |\{\sigma_i\}\rangle_A \otimes |-\{\sigma_i\}\rangle_B \end{aligned} \tag{4}$$

(where the sum is over all configurations of spins σ_i on the lattice sites), which is a maximally entangled state between systems A and B. We will first consider one exact limit of the setup in which the maximal entanglement is most manifest, and then we will interpolate between this limit and the original setup.

We begin with one limit in which we show that the induced spin state in system B is exactly the Gutzwiller projection of the Chern insulator ground state. In this limit, instead of the local Kondo coupling, we consider a coupling that directly projects onto the maximally entangled state $|\Psi_{AB}\rangle$ (“global projector”). The composite Hamiltonian is thus

$$H = H_{v=1}(c_\uparrow) + H_{v=1}(c_\downarrow) - g |\Psi_{AB}\rangle \langle \Psi_{AB}| \tag{5}$$

To lowest order in degenerate perturbation theory in the coupling $g \geq 0$, the effective Hamiltonian for system B is given by

$$\langle \Psi_B | H_{\text{eff}}^B | \Psi_B \rangle = -g \langle \Psi_A^0 \otimes \Psi_B | \Psi_{AB} \rangle \langle \Psi_{AB} | \Psi_A^0 \otimes \Psi_B \rangle$$

where $\Psi_A^0 = |v_\uparrow = 1\rangle \otimes |v_\downarrow = 1\rangle$ is the Chern insulator ground state of A, and Ψ_B, Ψ_B' are arbitrary states in B. However, $|\Psi_{AB}\rangle$ only

involves states from system A with one fermion per site (see Eq. 4), and thus

$$\langle \Psi_B' | H_{\text{eff}}^B | \Psi_B \rangle = -g \langle \Psi_A^s \otimes \Psi_B' | \Psi_{AB} \rangle \langle \Psi_{AB} | \Psi_A^s \otimes \Psi_B \rangle \quad (6)$$

where Ψ_A^s is the Gutzwiller projection of the Chern insulator ground state Ψ_A^0 , which, in turn, is a CSL.

Now, because Ψ_{AB} is a maximally entangled state (the reduced density matrix is the unit matrix), it can be expressed via a Schmidt decomposition as

$$|\Psi_{AB}\rangle = \frac{1}{\sqrt{2^N}} \sum_I |\alpha_I\rangle_A \otimes |\tilde{\alpha}_I\rangle_B \quad (7)$$

for any orthonormal basis $\{|\alpha_I\rangle_A\}$ of the spin sector (one fermion per site) of system A. Here, $|\tilde{\alpha}_I\rangle_B \equiv \sqrt{2^N} \langle \alpha_I | \Psi_{AB} \rangle$ is the corresponding basis for system B. For $|\Psi_{AB}\rangle$, the product state of singlets, it is clear that when written in the basis $|\alpha_I\rangle_A = |\{\sigma_i\}\rangle_A$ used in Eq. 4, $|\tilde{\alpha}_I\rangle_B = \Theta |\alpha_I\rangle_B$, where Θ is the time-reversal operator. However, it is straightforward (see Methods) to show that this statement holds in any basis $\{|\alpha_I\rangle_A\}$ of the spin sector (one fermion per site) of system A. Thus, choosing a basis $\{|\alpha_I\rangle_A\}$ of which Ψ_A^s , the Gutzwiller-projected ground state of A, is an element, Eqs. 6 and 7 yield

$$H_{\text{eff}}^B = -g |\overline{\Psi_B^s}\rangle \langle \Psi_B^s| \quad (8)$$

where $|\overline{\Psi_B^s}\rangle$ is the time-reversed counterpart of the Gutzwiller-projected Chern insulator ground state: It is a CSL with chirality opposite to the parent Chern insulator. Note that H_{eff}^B projects onto a single state—one of two degenerate ground states if the CSL were placed on a torus. However, on contractible regions (which we will consider below), there is no topological degeneracy, and the global projector projects onto the unique ground state.

Although the original Kondo coupling \hat{H}_K is a sum of local projectors onto a spin singlet (one at each lattice site i), we can interpolate between the exact limit of the global projector used in Eq. 5 and the local projector appearing in the original Kondo interaction term \hat{H}_K of Eq. 2. In particular, we partition systems A and B into regions r of linear dimension $l > \xi$, where ξ is the correlation length of A, and consider the quasi-local projector $P_r = -g |\Psi_{AB,r}\rangle \langle \Psi_{AB,r}|$ onto the product state of singlets supported in region r (see Fig. 2). $|\Psi_{AB,r}\rangle$ is analogous to Eq. 4, but the product over lattice sites “ i ” is constrained to a region r

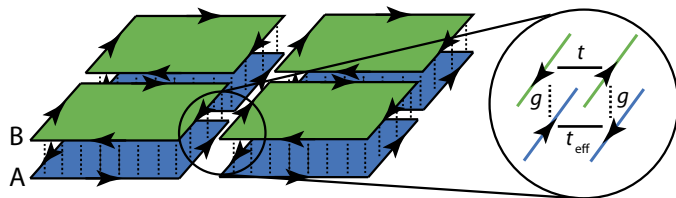


Fig. 2. Interpolation from global to local coupling. Systems A and B are each partitioned into regions. Corresponding regions r in A and B are coupled via a projection P_r onto the maximally entangled state of the two regions (dotted lines). If adjacent A regions are decoupled, as shown on the left, then each region of the Chern insulator induces a region of CSL via Eq. 8. Once the A regions are recoupled, adjacent edge states gap out, and the regions merge into a large Chern insulator. These interactions induce analogous interactions in B (inset), which fuse the B regions into a large CSL.

of linear size l . The sum over these quasi-local projectors, multiplied by $(-g)$, now replaces the global projector term in Eq. 5. Note that the local Kondo interaction term at a lattice site i in Eq. 2 is equal to the projector P_r in the limit where the region r comprises only one lattice site (hence, $r = i$, and $l = a =$ one lattice spacing).

First, we consider turning off the interactions $H_{rr'}^A$ between adjacent regions r, r' in A. Each region of the Chern insulator in A gives rise to a corresponding region of CSL in B via the projector P_r , as shown in Fig. 2. The low-energy states are the chiral (antichiral) edge modes of layers A and B, weakly coupled by an interlayer interaction of order g . However, once the interaction $H_{rr'}^A$ between adjacent regions r and r' in region A is restored, the thereby generated coupling between adjacent edge states within A stitches the Chern insulator back together. At the same time, $H_{rr'}^A$ induces, via the interlayer coupling, a corresponding interaction $H_{rr'}^B$ in layer B (see Fig. 2, inset) that gaps out adjacent edge states in B, thus creating a CSL state in the whole of system B.

By choosing finer and finer partitions, this construction interpolates between the global projector and the local projector considered in the primary model. Allowing for the full extent of interpolation requires as small a correlation length ξ for system A as possible, because the linear size of the quasi-local projectors is limited by ξ . Although the original model with a local Kondo coupling is an extreme limit of this interpolation, we note that the strength of the coupling g serves as an additional parameter that can also interpolate between the global and local projectors; the larger g is, the more both projectors favor the maximally entangled state. Nevertheless, the validity of this picture for the local Kondo coupling model ultimately requires further analysis for specific lattice models, which we now present.

Z_2 spin liquids from superconductors

We first present an exactly solvable example for the entanglement argument provided in the previous section. In particular, we consider an example in which the parent system (layer A) is a free-fermion superconductor with zero correlation length, for which we can analytically show that the topological bootstrap (with local Kondo coupling) gives rise to a Z_2 spin liquid—the Gutzwiller projection of the free-fermion superconductor, predicted by the entanglement argument of the previous section. The effective Hamiltonian induced in B is exactly the toric code (22, 23).

Let system A be a square lattice with four Majorana modes per site i , labeled $\gamma_i^{[\pm x]}, \gamma_i^{[\pm y]}$ (see Fig. 3), where $\{\gamma_i^{(\mu)} \gamma_j^{(\nu)}\} = 2\delta_{ij} \delta_{\mu,\nu}$. System B consists of spin- $\frac{1}{2}$ degrees of freedom \vec{S}_i at each site i of the square lattice. We choose an arrow convention on the links of the square lattice so that arrows are always directed along the $+x(y)$ direction for horizontal (vertical) links (see Fig. 3).

We consider the following Hamiltonian

$$H = H_A + H_{AB} \quad (9)$$

$$H_A = \sum_i \sum_{\mu=+x,+y} i\gamma_i^{[\mu]} \gamma_{i+\mu}^{[-\mu]} \quad (10)$$

$$H_{AB} = g \sum_{i,\alpha,\beta} \vec{S}_i \cdot (c_{i,\alpha}^\dagger \vec{\sigma}_{\alpha\beta} c_{i,\beta}) \quad (11)$$

$$c_{i,\uparrow} = \frac{\gamma_i^{[-x]} + i\gamma_i^{[+x]}}{2}, \quad c_{i,\downarrow} = \frac{\gamma_i^{[+y]} + i\gamma_i^{[-y]}}{2} \quad (12)$$

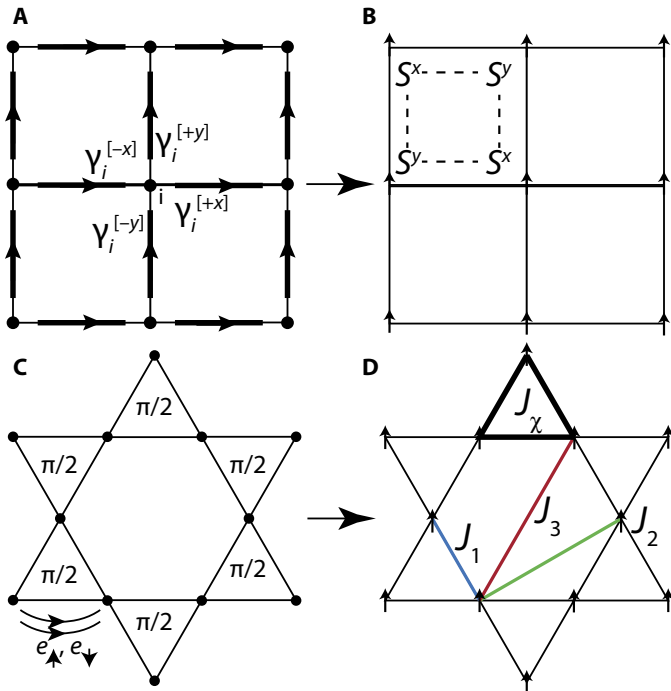


Fig. 3. Topological bootstrap in lattice models. (A) Free-fermion superconductor. Each site has four Majorana fermions, which form directed dimers (bold, with arrows) on the links with neighboring modes. (B) The superconductor induces the Wen plaquette/toric code via Kondo coupling. (C) Chern insulator on the kagome lattice realized from nearest-neighbor hopping of spin-up and spin-down electrons with a background $\pi/2$ flux per triangle. (D) The Chern insulator induces a CSL via Kondo coupling, with exchange and chirality parameters given in Eq. 15.

The ground state of H_A features dimerized Majorana fermions on every link (Fig. 3): This is a free-fermion topological superconductor with gapless Majorana edge states protected by translation symmetry [cutting through a rung of dimers exposes unpaired Majorana modes, which must be gapless given the translation symmetry along the cut (24)]. The term H_{AB} represents an exchange coupling with the initially decoupled spin- $\frac{1}{2}$ degrees of freedom of layer B.

At lowest order in g in degenerate perturbation theory, one finds that the induced spin Hamiltonian in layer B is

$$H_B^{\text{eff}} \propto g^4 \sum_i S_i^y S_{i+x}^x S_{i+x+y}^y S_{i+y}^x \quad (13)$$

which is the Wen plaquette model (23) with Z_2 topological order, equivalent to the toric code (22) by a basis change. As discussed by Wen (23), the ground state of this model is the projection of the Majorana dimer wave function onto the sector with $\gamma_i^{[+y]} \gamma_i^{[+x]} \gamma_i^{[-x]} \gamma_i^{[-y]} = 1$ for every site i , which corresponds to the single-occupancy constraint $\sum_{\sigma} c_{i,\sigma}^\dagger c_{i,\sigma} = 1$. This solvable example with zero correlation length is a direct illustration of the entanglement argument provided in the previous section.

CSLs from Chern insulators

We expect the above physics to persist when the correlation length of the A system is small but finite, and we now confirm this expect-

tation with two lattice models. First, we consider a model on the kagome lattice with a Hamiltonian of the form of Eq. 2 and explicitly derive the spin Hamiltonian induced by the Chern insulator to leading order in the Kondo coupling g .

We use a tight-binding model (25) of fermions with nearest-neighbor hopping in a background flux of ϕ through each triangle and $\pi - 2\phi$ through each hexagon (see Fig. 3). The hopping amplitude is set to 1. When $\phi = 0, \pi$, the band structure is gapless with two Dirac cones at low energy. By taking $\phi = \pi/2$, a nontrivial gap is opened with a Chern number 1 ground state.

The effective spin Hamiltonian is constrained by $SU(2)$ spin rotation and lattice symmetries to be of the form

$$H_{\text{eff}}^B = \sum_{ij} J_{ij} \vec{S}_i \cdot \vec{S}_j + \sum_{ijk} J_{ijk} \vec{S}_i \cdot (\vec{S}_j \times \vec{S}_k) + \dots \quad (14)$$

where higher-order spin interactions have been neglected because they are suppressed by powers of g . Furthermore, because the fermionic system in layer A is gapped, the induced spin interactions in layer B will decay exponentially with distance, and we can restrict attention to nearest neighbors for both the two-spin Heisenberg interaction and the three-spin “chirality” term, which requires broken time-reversal symmetry. Following the convention of previously considered kagome spin models, we will denote the relevant two-spin couplings by J_1, J_2, J_3 (nearest, next-nearest, and third-nearest neighbor) and the triangular spin chirality term by J_χ (Fig. 3D).

These effective couplings can be attained from degenerate perturbation theory in g (see the Supplementary Materials), and for the above model, we find, after normalizing J_1 to 1

$$J_1 = 1, \quad J_2 = 0.51, \quad J_3 = 0.56, \quad J_\chi = -0.49g \quad (15)$$

First, we consider $0 < g < 1$, for which J_χ can be ignored: A density matrix renormalization group (DMRG) study (26) established the CSL phase in the parameter range $0.1J_1 < J_2 = J_3 < 0.7J_1$, and a subsequent variational Monte Carlo study (27) revealed that the CSL phase persists for $J_3 > J_2$. Hence, the effective spin Hamiltonian from our model lies within the CSL phase.

For larger g , the next leading order contribution is the chirality term J_χ . The DMRG analysis by Bauer *et al.* (28) has shown that the spin model with J_χ alone is a CSL and that this phase persists even after including a nearest-neighbor term as large as $J_1 \approx 6J_\chi$. Thus, the CSL phase is reinforced by the higher-order chirality term.

The topological induction of the kagome CSL serves as a demonstration of concept for our construction, and we can apply it to many different lattices. For example, consider a similar setup on the triangular lattice, in which there is also a simple tight-binding Hamiltonian realizing a Chern insulator with Chern number 1: nearest-neighbor hopping with a uniform $\pi/2$ flux through each triangle. We use the same technique as above to derive the effective spin Hamiltonian (Eq. 14) that is induced, and we find at lowest order in g

$$J_1 = 1, \quad J_2 = 0.064, \quad J_3 = -0.018, \quad J_\chi = -0.25g$$

With J_1, J_2 alone, a DMRG study (29) found evidence for a gapped spin liquid in the regime $0.06 < J_2/J_1 < 0.17$, whereas another DMRG

study (30) has found spin liquids in the regime $0.07 < J_2/J_1 < 0.15$, with evidence of broken time-reversal symmetry. To our knowledge, the nature of the spin liquid(s) in this regime has not been fully settled. A more recent DMRG study finds that an additional spin chirality term J_χ as small as $0.02J_1$ can stabilize the CSL, and a variational Monte Carlo study (31) also advocates the role of the chirality term in stabilizing the CSL. Finally, a recent exact diagonalization study (32) also indicates that given the above J_2 , a small chirality term favors the CSL. These numerical studies indicate that our model at small but finite g is in the CSL phase.

DISCUSSION

We have provided a powerful machinery to obtain intrinsic topological orders, such as the Z_2 and the CSLs, from experimentally more easily accessible free-fermion phases, such as superconductors and Chern insulators. General arguments involving the topological proximity effect and entanglement, as well as explicit lattice models treated analytically and numerically, support this induction of intrinsic topological orders via Kondo coupling to a free-fermion phase. Two elements are essential for this topological bootstrap. On the one hand, the bulk topological proximity effect provides a mechanism of inducing the inverse topological phase of the parent system. On the other hand, the fact that the secondary system only hosts spin degrees of freedom forces the induction to be restricted to the spin sector of the parent system, hence realizing the Gutzwiller-projected free-fermion states as the ground state of the spin system.

The maximally entangled state of local singlets thus serves as a channel through which the spin sector of a noninteracting system of fermions can be inverted and filtered into the localized spin system. There are many directions to explore this topological bootstrap scheme, including different lattices, higher dimensions, different parent free-fermion phases, and alternative coupling schemes. Our construction provides both a physical route toward realizing phases with intrinsic topological order in synthetic composite systems, such as ultracold atoms, and a numerical route for deriving microscopic spin Hamiltonians that realize QSLs. The latter may, in turn, guide the search for solid-state materials that realize spin liquids or may provide relatively simple models that can be implemented to realize synthetic spin liquids. Because the Gutzwiller projection of higher-Chern number states results in non-abelian CSLs (14), it would be interesting to use the topological bootstrap to generate lattice models of these non-abelian phases.

METHODS

We show that for the product state of singlets

$$|\Psi_{AB}\rangle = \prod_i \frac{1}{\sqrt{2}} \left(c_{i,\uparrow}^\dagger |0\rangle \otimes |S_i^z = \downarrow\rangle - c_{i,\downarrow}^\dagger |0\rangle \otimes |S_i^z = \uparrow\rangle \right) \quad (16)$$

the Schmidt decomposition

$$|\Psi_{AB}\rangle = \frac{1}{\sqrt{N}} \sum_i |\alpha_i\rangle_A \otimes |\tilde{\alpha}_i\rangle_B \quad (17)$$

has the property that $|\tilde{\alpha}_i\rangle_B = \Theta |\alpha_i\rangle_B$, where Θ is the time-reversal operator, for any orthonormal basis $\{|\alpha_i\rangle_A\}$.

First, notice that choosing the basis $\{|\alpha_i\rangle_A\}$ to be product states of up and down spins, the above statement is manifest because it holds for each singlet.

Now, let $\{|\beta_i\rangle_A\}$ be any orthonormal basis. Then, its corresponding state in the Schmidt decomposition is

$$|\tilde{\beta}_i\rangle_B = \langle \beta_i | \Psi_{AB} \rangle \quad (18)$$

$$= \sum_j \langle \beta_i | \alpha_j \rangle_A \Theta |\alpha_j\rangle_B \quad (19)$$

$$= \sum_j \Theta \langle \alpha_j | \beta_i \rangle_A |\alpha_j\rangle_B \quad (20)$$

$$= \Theta \sum_j |\alpha_j\rangle_B \langle \alpha_j | \beta_i \rangle_B \quad (21)$$

$$= \Theta |\beta_i\rangle_B \quad (22)$$

(In Eq. 21, the matrix elements can be taken in either the A or the B system.)

SUPPLEMENTARY MATERIALS

Supplementary material for this article is available at <http://advances.sciencemag.org/cgi/content/full/3/10/e1700729/DC1>

Derivation of effective spin Hamiltonians for CSL

fig. S1. Convergence in two-spin interaction coefficient as a function of mesh linear dimension.

fig. S2. Convergence in spin chirality strength as a function of mesh linear dimension.

REFERENCES AND NOTES

1. X. Chen, Z.-C. Gu, Z.-X. Liu, X.-G. Wen, Symmetry protected topological orders and the group cohomology of their symmetry group. *Phys. Rev. B* **87**, 155114 (2013).
2. F. Pollmann, A. Turner, E. Berg, M. Oshikawa, Entanglement spectrum of a topological phase in one dimension. *Phys. Rev. B* **81**, 064439 (2010).
3. Z.-C. Gu, X.-G. Wen, Tensor-entanglement-filtering renormalization approach and symmetry-protected topological order. *Phys. Rev. B* **80**, 155131 (2009).
4. X.-G. Wen, Topological orders in rigid states. *Int. J. Mod. Phys. B* **04**, 239 (1990).
5. M. Z. Hasan, C. L. Kane, *Colloquium: Topological insulators. Rev. Mod. Phys.* **82**, 3045–3067 (2010).
6. L. Fu, Topological crystalline insulators. *Phys. Rev. Lett.* **106**, 106802 (2011).
7. T. H. Hsieh, H. Lin, J. Liu, W. Duan, A. Bansil, L. Fu, Topological crystalline insulators in the SnTe material class. *Nat. Commun.* **3**, 982 (2012).
8. D. Tsui, H. L. Stormer, A. C. Gossard, Two-dimensional magnetotransport in the extreme quantum limit. *Phys. Rev. Lett.* **48**, 1559–1562 (1982).
9. L. Balents, Spin liquids in frustrated magnets. *Nature* **464**, 199–208 (2010).
10. C. Nayak, S. H. Simon, A. Stern, M. Freedman, S. Das Sarma, Non-Abelian anyons and topological quantum computation. *Rev. Mod. Phys.* **80**, 1083–1159 (2008).
11. A. Yu. Kitaev, Fault-tolerant quantum computation by anyons. *Ann. Phys.* **303**, 2–30 (2003).
12. P. W. Anderson, The resonating valence bond state in La_2CuO_4 and superconductivity. *Science* **235**, 1196–1198 (1987).
13. C. Gros, Physics of projected wavefunctions. *Ann. Phys.* **189**, 53 (1989).
14. X.-G. Wen, Projective construction of non-Abelian quantum Hall liquids. *Phys. Rev. B* **60**, 8827–8838 (1999).
15. X.-G. Wen, Quantum orders and symmetric spin liquids. *Phys. Rev. B* **65**, 165113 (2002).
16. P. A. Lee, N. Nagaosa, X.-G. Wen, Doping a Mott insulator: Physics of high-temperature superconductivity. *Rev. Mod. Phys.* **78**, 17–85 (2006).
17. T. H. Hsieh, H. Ishizuka, L. Balents, T. L. Hughes, Bulk topological proximity effect. *Phys. Rev. Lett.* **116**, 086802 (2016).
18. T. Hsieh, Entangled cloning of stabilizer codes and free fermions. *Phys. Rev. B* **94**, 161112(R) (2016).
19. V. Kalmeyer, R. B. Laughlin, Equivalence of the resonating-valence-bond and fractional quantum Hall states. *Phys. Rev. Lett.* **59**, 2095–2098 (1987).

20. X. G. Wen, F. Wilczek, A. Zee, Chiral spin states and superconductivity. *Phys. Rev. B* **39**, 11413–11423 (1989).
21. A. E. B. Nielsen, G. Sierra, J. I. Cirac, Local models of fractional quantum Hall states in lattices and physical implementation. *Nat. Commun.* **4**, 2864 (2013).
22. A. Kitaev, Anyons in an exactly solved model and beyond. *Ann. Phys.* **321**, 2–111 (2006).
23. X.-G. Wen, Quantum orders in an exact soluble model. *Phys. Rev. Lett.* **90**, 016803 (2003).
24. T. H. Hsieh, G. B. Halász, T. Grover, All Majorana models with translation symmetry are supersymmetric. *Phys. Rev. Lett.* **117**, 166802 (2016).
25. M. Hermele, Y. Ran, P. A. Lee, X.-G. Wen, Properties of an algebraic spin liquid on the kagome lattice. *Phys. Rev. B* **77**, 224413 (2008).
26. S.-S. Gong, W. Zhu, D. N. Sheng, Emergent chiral spin liquid: Fractional quantum Hall effect in a kagome Heisenberg model. *Sci. Rep.* **4**, 6317 (2014).
27. W.-J. Hu, W. Zhu, Y. Zhang, S. Gong, F. Becca, D. N. Sheng, Variational Monte Carlo study of a chiral spin liquid in the extended Heisenberg model on the kagome lattice. *Phys. Rev. B* **91**, 041124 (2015).
28. B. Bauer, L. Cincio, B. P. Keller, M. Dolfi, G. Vidal, S. Trebst, A. W. W. Ludwig, Chiral spin liquid and emergent anyons in a Kagome lattice Mott insulator. *Nat. Commun.* **5**, 5137 (2014).
29. Z. Zhu, S. R. White, Spin liquid phase of the $S = \frac{1}{2} J_1 - J_2$ Heisenberg model on the triangular lattice. *Phys. Rev. B* **92**, 041105 (2015).
30. W.-J. Hu, S.-S. Gong, W. Zhu, D. N. Sheng, Competing spin-liquid states in the spin- $\frac{1}{2}$ Heisenberg model on the triangular lattice. *Phys. Rev. B* **92**, 140403 (2015).
31. W.-J. Hu, S.-S. Gong, D. N. Sheng, Variational Monte Carlo study of chiral spin liquid in quantum antiferromagnet on the triangular lattice. *Phys. Rev. B* **94**, 075131 (2016).
32. A. Wietek, A. M. Läuchli, Chiral spin liquid and quantum criticality in extended $S = \frac{1}{2}$ Heisenberg models on the triangular lattice. *Phys. Rev. B* **95**, 035141 (2017).

Acknowledgments: We thank S.-S. Gong, T. Grover, W.-J. Hu, and H.-H. Lai for useful discussions. **Funding:** T.H.H. was supported by the Gordon and Betty Moore Foundation's Emergent Phenomena in Quantum Systems Initiative through grant GBMF4304. Y.-M.L. was supported by start-up funds at Ohio State University. A.W.W.L. was supported by NSF under grant no. DMR-1309667. We acknowledge the Kavli Institute for Theoretical Physics Program "Novel States in Spin-Orbit Coupled Quantum Matter" and the NSF under grant no. NSF PHY11-25915. **Author contributions:** All authors contributed to the development of the technique. **Competing interests:** The authors declare that they have no competing interests. **Data and materials availability:** All data needed to evaluate the conclusions in the paper are present in the paper and/or the Supplementary Materials. Additional data related to this paper may be requested from the authors.

Submitted 6 March 2017

Accepted 12 September 2017

Published 6 October 2017

10.1126/sciadv.1700729

Citation: T. H. Hsieh, Y.-M. Lu, A. W. W. Ludwig, Topological bootstrap: Fractionalization from Kondo coupling. *Sci. Adv.* **3**, e1700729 (2017).

Topological bootstrap: Fractionalization from Kondo coupling

Timothy H. Hsieh, Yuan-Ming Lu and Andreas W. W. Ludwig

Sci Adv 3 (10), e1700729.
DOI: 10.1126/sciadv.1700729

ARTICLE TOOLS

<http://advances.sciencemag.org/content/3/10/e1700729>

SUPPLEMENTARY MATERIALS

<http://advances.sciencemag.org/content/suppl/2017/10/02/3.10.e1700729.DC1>

REFERENCES

This article cites 32 articles, 1 of which you can access for free
<http://advances.sciencemag.org/content/3/10/e1700729#BIBL>

PERMISSIONS

<http://www.sciencemag.org/help/reprints-and-permissions>

Use of this article is subject to the [Terms of Service](#)

Science Advances (ISSN 2375-2548) is published by the American Association for the Advancement of Science, 1200 New York Avenue NW, Washington, DC 20005. The title *Science Advances* is a registered trademark of AAAS.

Copyright © 2017 The Authors, some rights reserved; exclusive licensee American Association for the Advancement of Science. No claim to original U.S. Government Works. Distributed under a Creative Commons Attribution NonCommercial License 4.0 (CC BY-NC).